

The Use of MathCad in Teaching Ideal Fluid Flow with Complex Variables*

MICHAEL REX MAIXNER

Maine Maritime Academy, Castine, Maine ME, USA. E-mail: mmaixner@bell.mma.edu

The use of MathCad for the visualization of two-dimensional, irrotational, steady, incompressible flow patterns is discussed, along with the appropriate mathematical background. MathCad's contour plotting capabilities and its ability to handle complex numbers permit rapid depiction of basic flows and linear combinations of these flows with relative ease, allowing students to concentrate on understanding the material and broader concepts. Sample output, recommended lecture topics, and suggested topics for further study are presented, and the address of a web site containing a prepared lecture is provided (<http://www.mathsoft.com/lappsindex.html>).

NOMENCLATURE

a	cylinder radius
f	complex function used in definition of Milne-Thompson circle theorem (see text)
F	$= \phi + i\psi$, complex potential
F'	$= \frac{dF}{dz} = u - i\hat{v}$, complex velocity
\bar{F}'	$= u + i\hat{v}$, velocity
\hat{i}	$= \sqrt{-1}$ (Note the carat (^) atop the letter i to differentiate it from the letter i when employed as a subscript or index.)
i	index associated with x-direction
j	index associated with y-direction
n	number of subdivisions in x- and y-directions
Q	array of source and sink strengths in von Kármán problem (see text)
r	$= z = \sqrt{x^2 + y^2}$, modulus of position in the complex plane
U_0	magnitude of free stream velocity
u	velocity in the x-direction
v	velocity in the y-direction
V	$= F' = \bar{F}' $, magnitude of velocity
x	real component of position in the complex plane
X	array of source and sink locations in von Kármán problem (see text)
y	imaginary component of position in the complex plane
z	$= x + iy = re^{i\theta}$, position in the complex plane
α	orientation angle of free-stream relative to positive x-axis
β	orientation angle of doublet relative to positive x-axis
Γ	vortex strength
θ	angle of position in the complex plane, measured counter-clockwise from positive x-axis

λ	source (or sink) strength
μ	doublet strength
ϕ	$= \text{Re}(F)$, potential function
ψ	$= \text{Im}(F)$, stream function

INTRODUCTION

FLOW VISUALIZATION has been an invaluable tool in the study of ideal and real fluid flows, providing a synergism that allows the student to gain an understanding not only of the phenomenological aspects of the flow, but also of the underlying mathematics. Detailed analysis of these flow visualizations permits not only the streamline and equipotential patterns to be obtained, but also the location of critical points in the flow, such as stagnation points. Numerous methods of flow visualization exist, and include electric analogs, experimental techniques (hydrogen bubble method, smoke tunnels, aluminum flakes sprinkled on the surface of dye-colored water, dye injection, etc. [1, 2]). Given the requisite time and patience, qualitative sketches of potential flow patterns provide additional insight into the underlying physics. A natural outgrowth of sketches is the use of computer graphics to assist in these visualizations, but early attempts at the use of computers for this purpose were generally limited to main-frame machines with, eventually, time-sharing workstations with graphics terminals [3–6]. More recent developments in flow visualization with personal computers are provided in the references [7–9]. MathCad, a relatively inexpensive and readily available calculation software product, combines an excellent contour plotting capability and the ability to perform calculations with complex functions. This makes it an extremely powerful tool in the visualization of ideal fluid flow patterns by individual users on personal computers.

* Accepted 6 June 1999.

Students with a background in basic fluid mechanics and complex variables are quickly able to obtain plots of streamlines and equipotential lines.

At Maine Maritime Academy, the course 'Numerical and Computer Methods for Engineering Design' (Es490) is taken in the spring term of the third year of a five-year marine engineering systems curriculum. Prior to that, students have had basic courses in fluid mechanics and structured computer programming, and will also have been introduced to complex variables. Es490 also follows an introductory design course, and is taken in conjunction with an intermediate design course. The course provides students with a variety of numerical methods and techniques (numerical integration, differentiation, finite difference methods, interpolation, curve fitting, solution of differential equations and systems of differential equations, etc.) that may be used throughout the remainder of their curriculum, including the two-semester capstone design sequence taken in the fifth year. Excel spreadsheets, QBASIC, and MathCad are utilized to complete a variety of problems (structural, electrical, fluid mechanics, optimization, aerodynamics, heat transfer, etc.).

As part of this course, students receive instruction in the representation of ideal fluid flows as a complex function whose real and imaginary parts are, respectively, the potential and stream functions. Following this basic instruction and several examples, students are required to solve problems involving linear combinations of these potential flows, to draw elementary conclusions from these representations, and, in general, to recognize the power of this method, especially when used in conjunction with boundary layer methods at fluid-structure interfaces. The prototype of this instructional method was employed in the early 1980s by the author when on the faculty of the Department of Mechanical Engineering at the Naval Postgraduate School in Monterey, California. At that time, an IBM 360 mainframe was required to run the program, with students utilizing time-sharing stations and separate Tektronix graphics screens to view the flow patterns. With the advent and proliferation of personal computers and software since then, the same capability is now available on desktop and laptop computers. The intent of this instructional package (originally at the Naval Postgraduate School and in its current incarnation at Maine Maritime Academy) was to relieve students of the laborious plotting associated with flow visualization. The student is thus able to investigate many more combinations of basic potential flows and, consequently, obtain a better understanding of the subject matter. It is this method and its specific implementation in Es490 at Maine Maritime Academy with which the remainder of this article is concerned.

BACKGROUND

Students who took the pilot version of Es490 in the fall of 1998 and spring of 1999 were required to purchase the student edition of MathCad, version 7. The professional edition of MathCad was also available for both classroom instruction and after-hours use on the local-area network. The topic of potential flows is presented in the latter part of the term, so students will already be familiar with MathCad when this subject is reached.

A detailed lesson plan file in MathCad worksheet format is provided to all students to follow along during the lectures and to use as a study guide. A copy of the lesson plan may be obtained through the MathCad web site or directly from the author by e-mail. Due to the number of illustrations embedded in the lesson plan and the grid size used for illustrations, it is recommended that the program be run on a computer with at least a Pentium processor, otherwise the refresh times for successive screens becomes excessively long. Alternatively, the grid coarseness may be increased by reducing the number of grid points (see next section) with a concomitant reduction in graphic quality.

The background for this topic may be found in various mathematics [10,11] and fluid mechanics [12] texts; many of the details are omitted here for the sake of brevity, but may be found in the lesson plan placed on the MathCad web site. Instruction begins with a review of the basics of complex number theory, whereby an imaginary number, z , may be represented in either rectangular (x - and y -components) or polar (r - and θ -components):

$$z = x + iy = re^{i\theta} = r(\cos \theta + i \sin \theta) \quad (1)$$

where $\theta = \arctan (y/x)$.

For the two-dimensional, irrotational, steady flow of an incompressible fluid, the u - and v -components of velocity (in the x - and y -directions, respectively) are related by the Cauchy-Riemann equations:

$$\begin{aligned} v &= -\frac{\partial \psi}{\partial x} = \frac{\partial \phi}{\partial y} \\ u &= \frac{\partial \psi}{\partial y} = \frac{\partial \phi}{\partial x} \end{aligned} \quad (2)$$

where ϕ and ψ are, respectively, the equipotential and stream functions for the flow; they are orthogonal, and give rise to the complex potential function:

$$F(z) = \phi(x, y) + i\psi(x, y) \quad (3)$$

Most students readily grasp the significance of a streamline (a line of constant ψ) and recognize that there can be no velocity normal to a streamline. The concept of an equipotential (a line of constant ϕ) is usually not as easily mastered, and must be reinforced through the correlation of the

Cauchy-Riemann equations with plots of equipotential lines in ideal flow patterns.

The student is then shown that the complex velocity may therefore be obtained from:

$$F'(z) = \frac{dF}{dz} = \frac{\partial F}{\partial x} = \frac{\partial \phi}{\partial x} + i \frac{\partial \psi}{\partial x} = u - iv \quad (4)$$

MathCad's built-in derivative function may be employed in this last equation. Note that in order to obtain the actual velocity, we must take:

$$\bar{F}'(z) = u + iv \quad (5)$$

Finally, the magnitude of the velocity may be obtained from:

$$V(z) = |F'(z)| = |\bar{F}'(z)| = [\bar{F}' \cdot F']^{1/2} = (u^2 + v^2)^{1/2} \quad (6)$$

DISCRETIZATION OF FLOW FIELD

Prior to displaying any of the more interesting potential flows, a grid must be established, with the grid intersections being the points at which ϕ and ψ will be calculated. A grid is employed with x and y each bounded by ± 1.5 , with the domain subdivided into a number of rectangles in the x - and y -directions. All grid points are then offset slightly by the same amount $x_{offset} = y_{offset} = 0.0001$; should the user decide to place a singularity at, say, $z = 0 + i0$, (a common choice), then calculation will not be performed 'at' the singularity. This shift is essentially transparent to the user from this point on. An equal number of grid points is utilized in each direction, with indices in the x - and y -directions, respectively, of $i = 0 \rightarrow n$ and $j = 0 \rightarrow n$; with $n = 25$, this gives, in all, $(n + 1)^2 = 676$ points in the plotting area. MathCad's default index counter is set to 0 so that all vector and matrix subscripts begin with 0; the grid point corresponding to $i = 0, j = 0$ is situated at the lower left corner of the plotting area.

The complex offset z_{offset} and complex grid-points $z_{i,j}$ are defined as:

$$\begin{aligned} z_{offset} &= x_{offset} + iy_{offset} \quad (7) \\ x_i &= x_{min} + \frac{i \cdot (x_{max} - x_{min})}{n} \\ y_j &= y_{min} + \frac{j \cdot (y_{max} - y_{min})}{n} \\ z_{i,j} &= z_{offset} + (x_i + iy_j) \end{aligned}$$

(The choice of z_{offset} and the grid size (i.e., n) may result in large values of $F(z)$, depending on how close a grid intersection lies to the location of a singularity. Since MathCad may arbitrarily select the contour values, adjacent contours may then appear very dense or very sparse. The user may be required to make judicious choices of n and the location of singularities to produce suitable contour density.)

Once the grid is established and ψ and/or ϕ are evaluated at each grid point, MathCad's contour plotting capability is used to plot ψ or ϕ . MathCad performs a linear interpolation between gridpoints to establish contours of the quantity being plotted (either ϕ or ψ); the ϕ_{ij} or ψ_{ij} are stored as a matrix of equally spaced values, without reference to the coordinates at which ϕ or ψ are evaluated. The default plotting limits for grid positions are $-1 \leq x \leq 1$ and $-1 \leq y \leq 1$, and must be changed by the user to reflect the values previously chosen (i.e., $x_{min} \leq x \leq x_{max}$ and $y_{min} \leq y \leq y_{max}$).

Version 7 of MathCad limits the user to one contour plot per graph. If, instead, two contour plots were allowed, then lines of constant ϕ and lines of constant ψ could be viewed on the same plot, thereby illustrating the orthogonality of these two functions. Instead, the user must plot ϕ and ψ on separate graphs; if placed in close proximity to one another, though, the orthogonality is readily discernable. MathCad Version 8 has enhanced three-dimensional and contour plotting capabilities, which allow the plotting of two sets of contours on the same graph.

BASIC FLOWS

With the preliminaries out of the way, the student is now introduced to the basic potential flows.

Free stream

A free stream of magnitude U_o and inclined at an angle to the positive x -axis of α will have the potential function:

$$F_{freestream}(z) = U_o z e^{-i\alpha} \quad (8)$$

Recalling that ϕ is the real part of the complex function, and that ψ is the imaginary part, we have $\phi_{i,j} = \text{Re}(F_{freestream}(z_{i,j}))$ and $\psi_{i,j} = \text{Im}(F_{freestream}(z_{i,j}))$. In the lesson plan, items such as α and U_o are included in the text as 'math regions' so that they may be varied as desired. In fact, the student is encouraged to do so, and to examine changes in the output – this is the real benefit of a program such as MathCad. As a consequence of the Cauchy-Riemann equations, the streamlines and equipotential lines are orthogonal for all potential flows and for all linear combinations of these flows. MathCad allows various modifications to the contour plots, including colors or shades of gray between successive contours, automatic contour plotting, choice of numbers of contours, etc. Figure 1 depicts the equipotential lines and streamlines for a free stream of magnitude $U_o = 1$ and $\alpha = \pi/3$.

Source/Sink

The complex potential for a source is given as:

$$F_{source}(z) = \frac{\lambda}{2\pi} \ln(z - z_{source}) \quad (9)$$

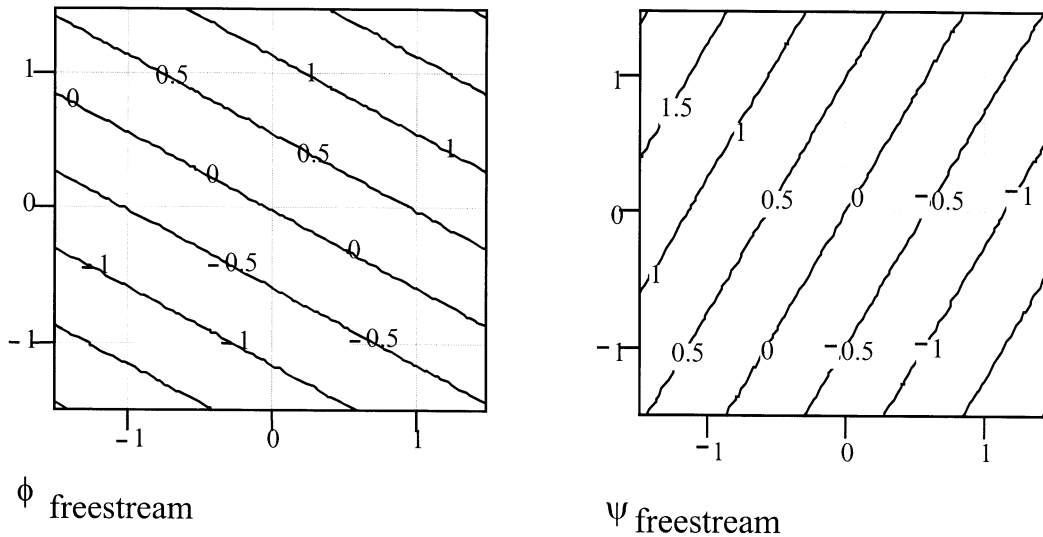


Fig. 1. Equipotentials and streamlines for free stream of strength $U_0 = 1$ and $\alpha = \pi/3$. Note the orthogonality of the two plots.

A sink is merely a source of negative strength. In Fig. 2 the equipotential lines and streamlines are plotted for a source of strength of $\lambda = 2\pi$ and located at $z_{source} = 0$, using the relations $\psi_{i,j} = \text{Im}(F_{source}(z_{i,j}))$ and $\phi_{i,j} = \text{Re}(F_{source}(z_{i,j}))$. Notice that the streamlines all emanate from the origin of the source, and that the equipotential lines and streamlines are everywhere perpendicular. Note also the concentrations of the streamlines along the negative x-axis – this is the location (within MathCad) of the so-called Riemann cut; the value of ψ jumps by a value of 2π as the Riemann cut is traversed.

Doublet

A doublet is formed when a source and sink of equal magnitude are brought together, maintaining the product of strength and separation at a constant value. In the limit, as the separation between the source and sink tends towards zero, a doublet of strength μ will result with an orienta-

tion relative to the positive x-axis of angle β (fluid emanating from the doublet on the side originally occupied by the source, and fluid entering the doublet on the side originally occupied by the sink); the complex potential is given as:

$$F_{doublet}(z) = \frac{-\mu e^{-i\beta}}{2\pi(z - z_{doublet})} \quad (10)$$

Equipotential lines and streamlines for a doublet at the origin and with strength $\mu = 2\pi$ and orientation $\beta = \pi$ are depicted in Fig. 3.

Vortex

For a vortex of strength Γ (a positive value of Γ results in a counter-clockwise velocity), the complex potential is:

$$F_{vortex}(z) = \frac{-i\Gamma}{2\pi} \ln(z - z_{vortex}) \quad (11)$$

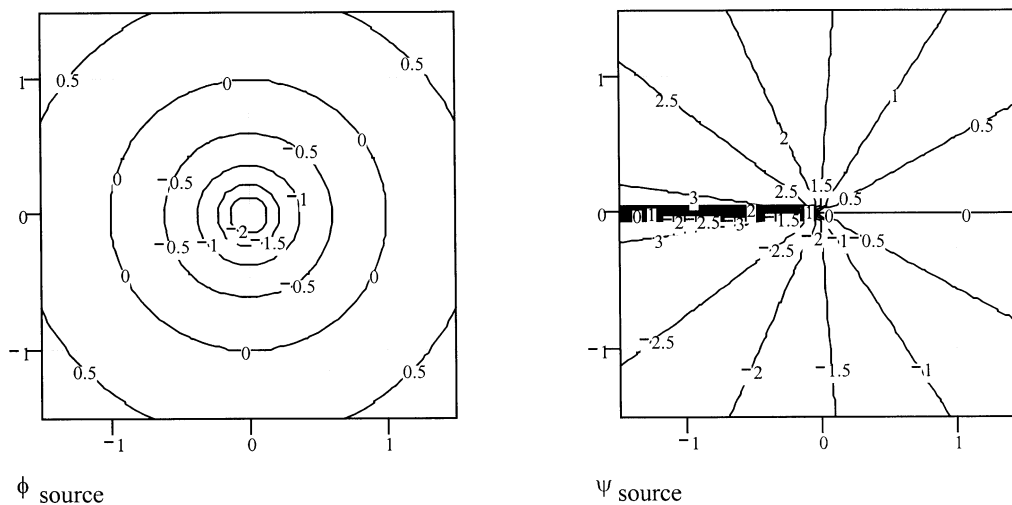


Fig. 2. Equipotentials and streamlines for source of strength $\lambda = 2\pi$.

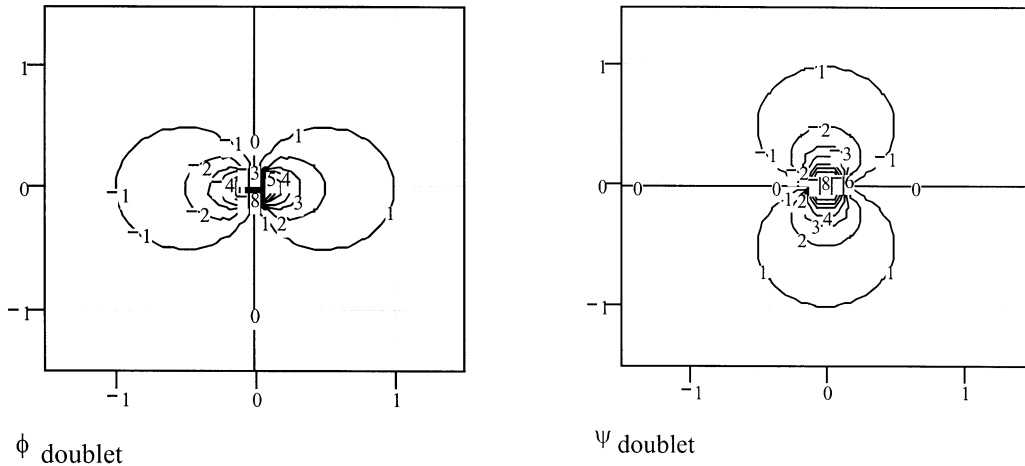


Fig. 3. Equipotentials and streamlines for a doublet of strength $\mu = 2\pi$ and orientation $\beta = \pi$.

Figure 4 depicts the equipotentials and streamlines for a vortex of strength $\Gamma = 2\pi$ situated at the origin. At this point, students are shown how the equipotentials for a source are analogous to the streamlines for a vortex, and vice-versa; this is due to the fact that their complex potentials are similar, differing only by a factor of $-i$.

toward the origin. Were a source used instead of a sink, the flow would spiral outward from the origin, much as is obtained in a centrifugal pump.

Aircraft trailing vortex system

When two vortices of equal magnitude, opposite sign, and located at z_1 and z_2 are combined, the following complex potential results:

COMBINATIONS OF BASIC FLOWS

'Bathtub' vortex

By combining a sink and a vortex, the following complex potential results:

$$F_{bathtub}(z) = -\frac{\lambda}{2\pi} \ln(z - z_{sink}) - \frac{i\Gamma}{2\pi} \ln(z - z_{vortex}) \tag{12}$$

$$F_{TV}(z) = \frac{-i\Gamma}{2\pi} [\ln(z - z_1) - \ln(z - z_2)] \tag{13}$$

$$= \frac{-i\Gamma}{2\pi} \ln\left(\frac{z - z_1}{z - z_2}\right)$$

Choosing $\lambda = \Gamma = 2\pi$ and $z_{sink} = z_{vortex} = 0$, a plot of the streamlines for this flow (Fig. 5) shows that the streamlines spiral, with the flow directed

Figure 6 depicts the streamlines obtained from two such vortices of magnitude 2π and situated $z = \pm 1$. In fact, what this situation represents is the flow pattern exhibited by a lifting wing, with a trailing vortex emanating from each wingtip. The vortices are 'images' of one another, and result in a plane of symmetry at mid-span ($x = 0$), where $\psi = 0$.

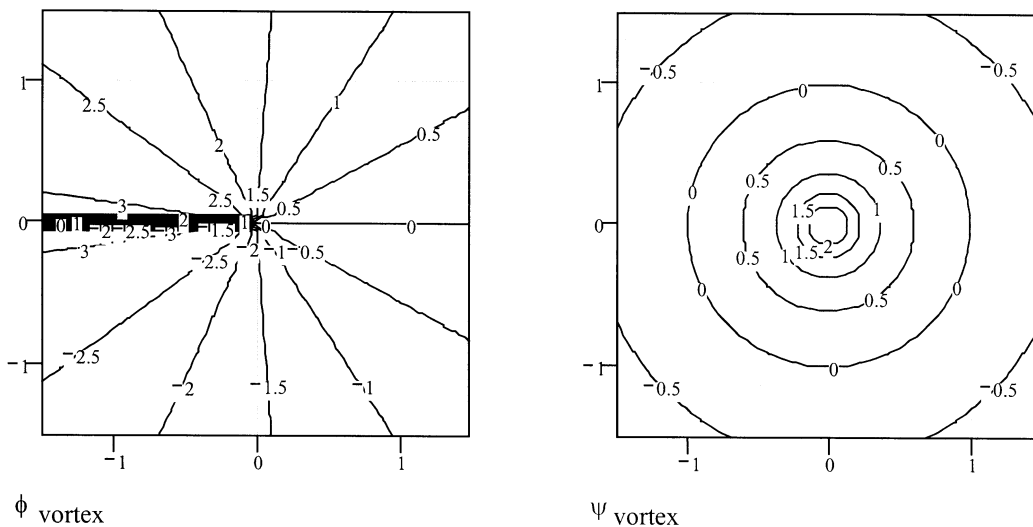
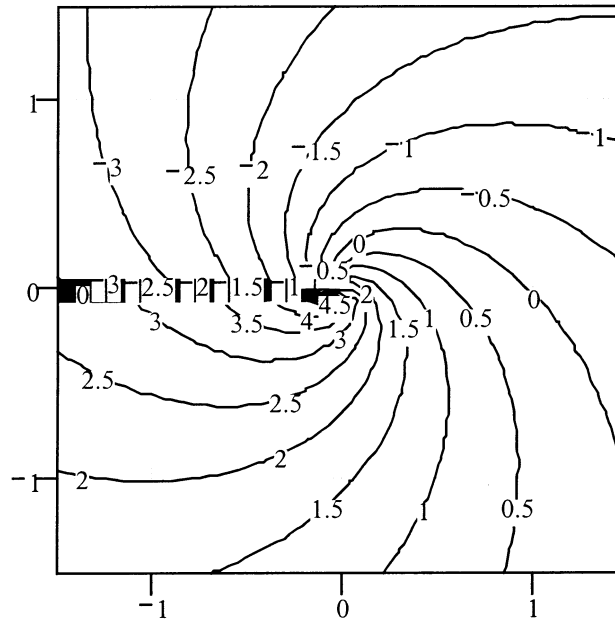


Fig. 4. Equipotentials and streamlines for vortex of strength $\Gamma = 2\pi$.



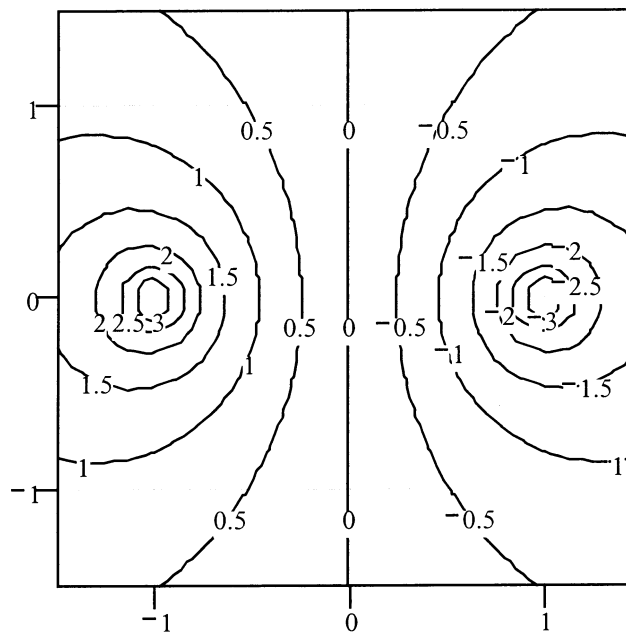
Ψ bathtub

Fig. 5. Streamlines for “bathtub” vortex.

The Magnus effect

In the early 1850’s, the Prussian army noted that rounds fired from their artillery pieces were falling long or short of the target, for no apparent reason. Gustav Magnus [13] was given the task of investigating this phenomenon. The bores of the artillery pieces were rifled to impart a spin to the rounds as they traversed the barrel to introduce stability to

the round after exiting the muzzle. Magnus discovered that when the projectiles were subjected to a crosswind in flight, the velocity on either the top or bottom of the spinning projectiles (depending on the wind’s direction) was augmented by the wind. This resulted in reduced pressure on that side of the projectile and a net force on the projectile in that direction. This tended to either keep the



Ψ trailing_vortex

Fig. 6. Streamlines resulting from aircraft trailing vortex system.

projectile aloft for a longer time (low pressure region on top) or a shorter time (low pressure region on the bottom). It is this same phenomenon which causes golf balls, baseballs, and other spinning spherical objects to deflect in flight [14]. (See the article by Swanson [15] for a more recent discussion of this effect.) The power of complex variables may be used to depict this region of higher velocity for the two-dimensional, rather than the three-dimensional case (i.e., the Magnus problem of a spinning cylinder, rather than a spinning sphere). This particular problem may be easily handled with MathCad.

Consider the combination of a freestream of magnitude $U_o = 1$ oriented $\alpha = 0$ (flow in the positive x-direction) and a doublet of strength $2\pi U_o$ oriented $\beta = \pi$ (in the negative x-direction) and situated at the origin. This results in a cylinder of unit radius whose surface is the locus of points where $\psi = 0$. Since there can be no flow through the surface of the cylinder (i.e. no normal velocity on the cylinder), the tangential velocity is the total velocity along this surface. We will also include a vortex of strength Γ at the origin – this will later be varied to investigate the effect of circulation on the flow pattern. The complex potential that results is:

$$F_{Magnus}(z) = U_o e^{-i\alpha} z - \frac{\mu e^{-i\beta}}{2\pi z} - \frac{i\Gamma}{2\pi} \ln z \quad (14)$$

With $\Gamma = 0$, the resulting streamline plot is shown in Fig. 7(a); stagnation points exist on the cylinder at the intersection of the cylinder surface with the x-axis. As the vortex circulation is increased to $\Gamma = -2\pi$ (i.e. circulation in a clockwise direction), the stagnation points move to locations on the lower two quadrants of the cylinder, as seen in Fig. 7(b). Further increasing the circulation to $\Gamma = -4\pi$ results in the stagnation points meeting at the bottom of the cylinder, Fig. 7(c), and a further increase results in one stagnation point moving *into* the flow, and the other moving *inside* the cylinder, Fig. 7(d)!

The region of more densely packed streamlines on the upper surface of the cylinder corresponds to a region of higher velocity since the free stream velocity adds to the rotational velocity imparted by the spinning cylinder. From Bernoulli's theorem, this is also a region of lower pressure, so that a net force in the positive y-direction results. At this point, a discussion of viscous effects and separation is appropriate, since the real flow would separate from the cylinder somewhere in the first quadrant (i.e. on the downstream side of the upper surface). It is also instructive to plot the velocity on the surface of the cylinder at several points for the ideal (i.e. unseparated) flow. A device employing this principle (a 26-meter high 'turbosail') will be installed as a means of supplementing more conventional means of propulsion on Calypso II, the research vessel for the Cousteau Society – it is anticipated that fuel savings on the order of 30 per

cent will be realized when compared to the fuel consumption of a more conventional vessel of the same size [16].

PROBLEMS FOR FURTHER STUDY

The basic flows and combinations thereof are contained in the lesson plan posted on the MathCad web site; the following constitute additional problems which may be employed as homeworks, projects, or to merely spark discussion.

Wing in ground effect

As an extension of the lifting wing problem, consider an aircraft in close proximity to the ground (i.e. during take-off or landing) [17, 18]. In addition to the plane of symmetry along the centerline of the aircraft discussed previously, there must now be another along the ground since there can be no flow through that plane either. The standard model of this is to add to each wingtip (located at z_1 and z_2) a vortex which must have an image of opposite sign situated as far *below* the ground (located at, respectively, z_4 and z_3) as the wingtip vortex is *above* the ground. The appropriate complex potential is;

$$F_{GE} = \frac{-i\Gamma}{2\pi} \ln \left[\frac{(z - z_1)(z - z_3)}{(z - z_2)(z - z_4)} \right] \quad (15)$$

The streamlines which result from a vortex strength of $\Gamma = 2\pi$, a wingspan of 2, and an altitude of one-quarter wingspan are depicted in Fig. 8(a). Since there can be no flow through the ground, the horizontal velocity there is the total velocity.

If positions along the ground are represented in complex number form and inserted in:

$$V_{ground}(z) = \left| \frac{d}{dz} F_{GE}(z) \right| \quad (16)$$

the velocities induced on the ground are obtained as in Fig. 8(b). It can be seen that the maximum induced velocities on the ground occur immediately beneath the real vortices. An additional topic that may be discussed is the path taken by the wingtip vortices after they are shed; the point must be made that each vortex (real or image) cannot induce any velocity on itself. Therefore, to calculate the velocity of a real vortex, the resulting complex potential must exclude the term corresponding to that vortex prior to calculating its velocity. The distance traveled by the vortex is then obtained via an Eulerian scheme over a suitably small time interval; the velocity is multiplied by the time interval, and this result is added to the previous position of that vortex to update its position. The other real vortex and the image vortices move a similar distance, but symmetrically relative to the aircraft centerline and the ground. The resulting path, Fig. 8(c), is hyperbolic, with the vortices moving toward the ground and outward.

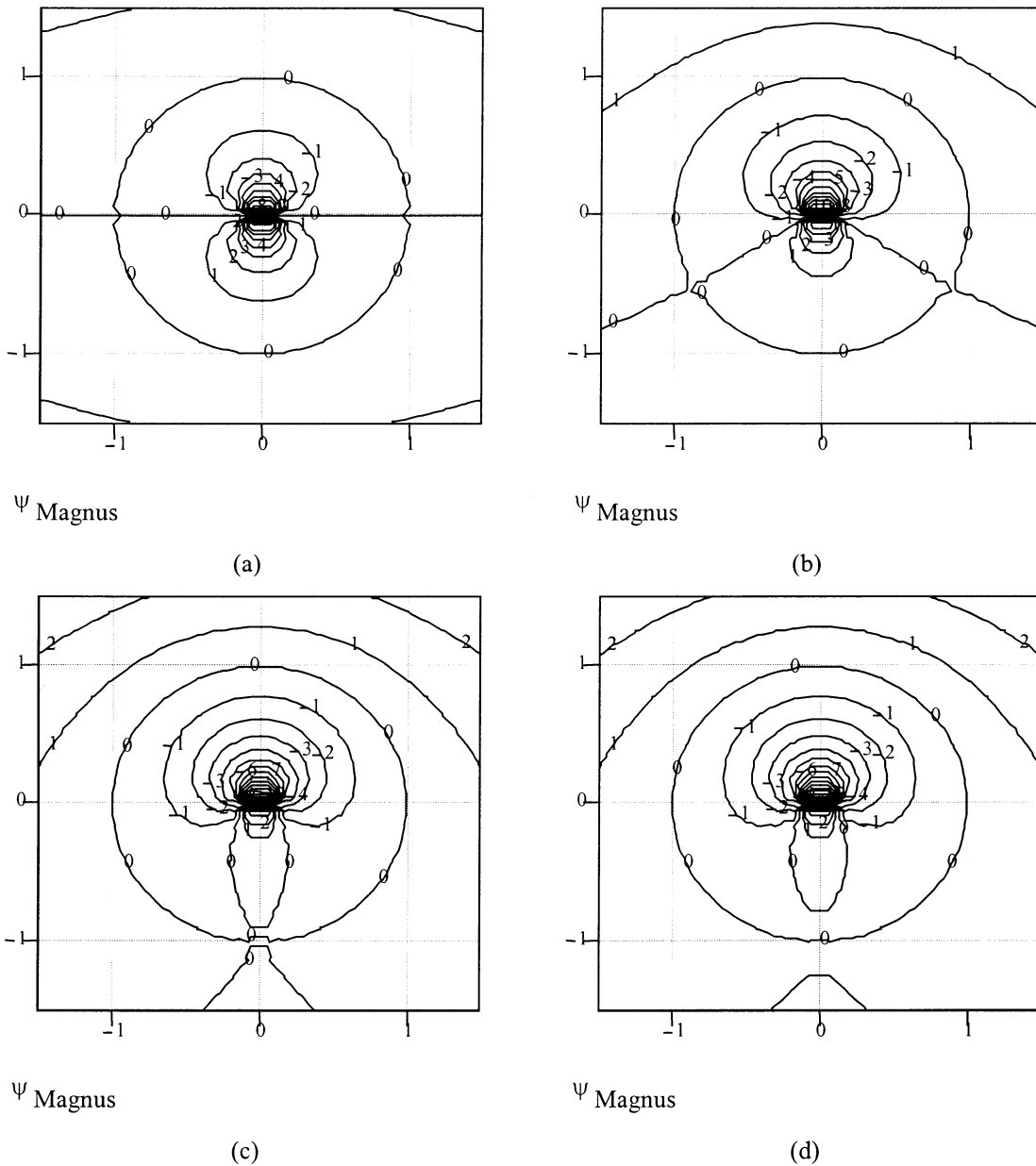


Fig. 7. Streamlines for flow about a cylinder with: (a) No circulation, with two stagnation points situated on x-axis; (b) Circulation of intermediate strength $\Gamma = -2\pi$, with two stagnation points moving down and towards each other; (c) Critical circulation of $\Gamma = -4\pi$, resulting in one stagnation point at the bottom of the cylinder; (d) Circulation of strength $\Gamma = -4.03\pi$, with one stagnation point moving towards the origin (inside cylinder) and the other in the flow moving away from the cylinder.

At this point, a discussion is appropriate of the effect that the trailing vortices shed by a large aircraft could have on smaller aircraft, and why there can be a significant wait on the ground as aircraft queue for take-off.

Von Kármán problem

In the 1920s, Theodore von Kármán was contracted by the Zeppelin company to investigate the pressure distributions on airship hulls. His ingenious method of combining various singularities to obtain the required airship body profiles, although created for the axisymmetric case, may be easily demonstrated with MathCad using combinations of the two-dimensional singularities

discussed above. For a detailed discussion of the method, see References [19–22].

Von Kármán’s method begins by placing a series of sources towards the bow along the centerline (i.e. the x-axis) of the body, and a series of sinks on the centerline towards the stern. The body is presumed to be operating head-on into a free stream of magnitude U_∞ . The sum of all sources should equal the sum of all sinks, so that there will not be any flow through the body. What is required is the proper combination of source and sink strengths and locations so that the body’s outline is matched by the $\psi = 0$ streamline.

A drawback of MathCad (before version 8) is that no other plot may be superposed on a contour

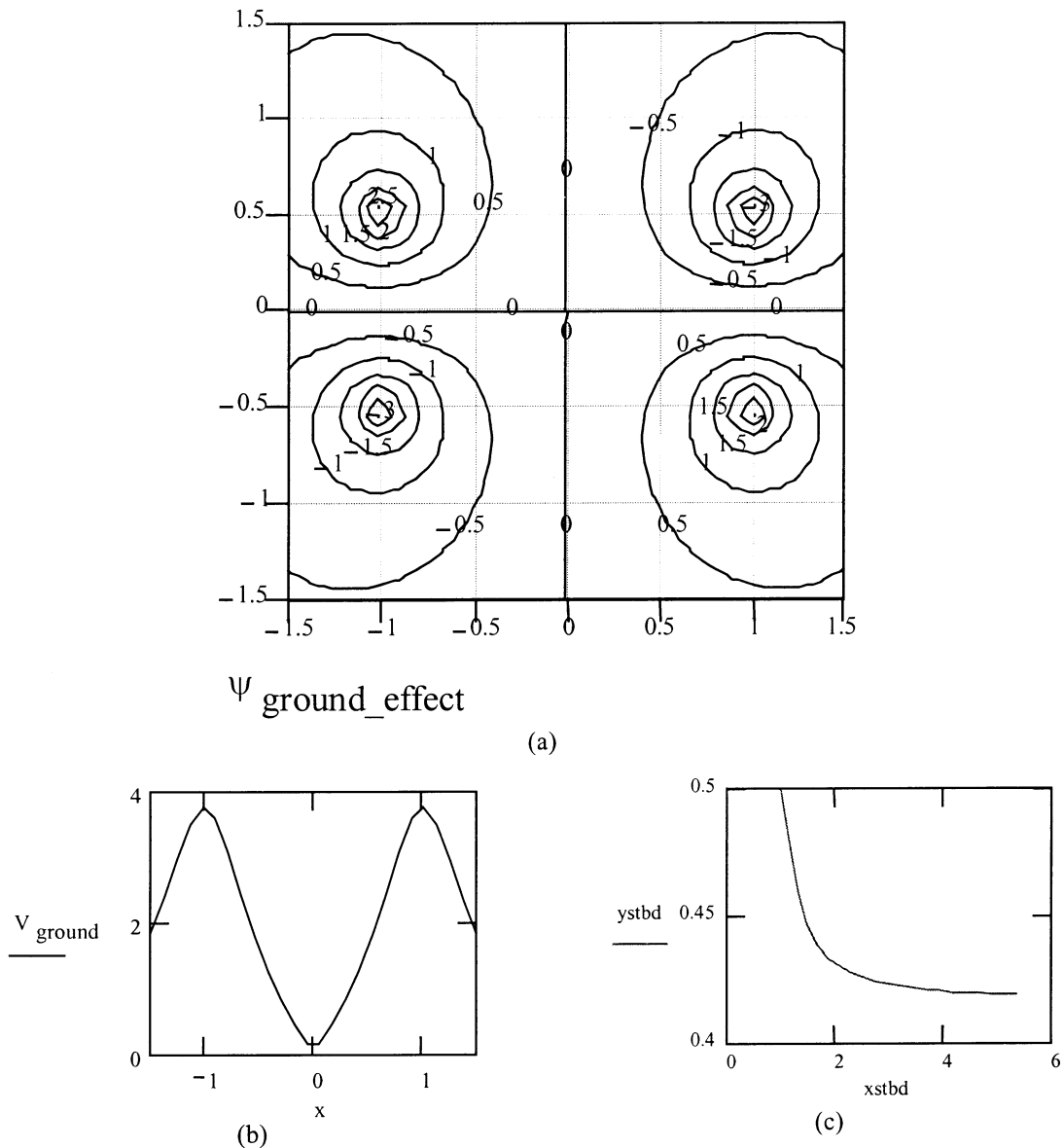


Fig. 8. (a) Streamlines resulting from aircraft in ground effect; (b) Velocities induced on ground; (c) Path of vortex shed from starboard wingtip.

plot. (Version 8 of Mathcad supports multiple plots of different types, as well as multiple contour plots.) Consequently, an ellipse or other outline which represents the airship hull may not be placed on a plot, so that the $\psi = 0$ streamline may be compared to it as singularities are changed. Instead, the student may be told to make the $\psi = 0$ streamline touch certain points on the x- and y-axes. Specifically, a combination of sources and sinks situated in a free stream is required which will place the $\psi = 0$ streamline at $y = \pm 0.75$ and $x = \pm 1.25$. An array Q containing the strengths of three sources and three sinks is used, along with an array X which contains the x-coordinates of the singularities. These will be used in the complex potential:

$$F_{VK}(z) = U_0z + \frac{1}{2\pi} \sum_{source} \ln(z - X_{source}) \quad (17)$$

Figure 9 depicts the streamlines obtained from:

$$Q = \begin{bmatrix} 0.8 \\ 1.0 \\ 0.9 \\ -0.9 \\ -1.0 \\ -0.8 \end{bmatrix} \quad \text{and} \quad X = \begin{bmatrix} -1.0 \\ -0.9 \\ -0.8 \\ 0.8 \\ 0.9 \\ 1.0 \end{bmatrix} \quad (18)$$

As the student varies any of the singularity parameters, the MathCad plot immediately updates itself and provides instantaneous feedback regarding the effect of each change. Outlines of actual airships are, in fact, not nearly as blunt as the outline depicted in Fig. 9; suitable choices of source and sink locations and strengths in the Q- and X-arrays could provide more realistic shapes.

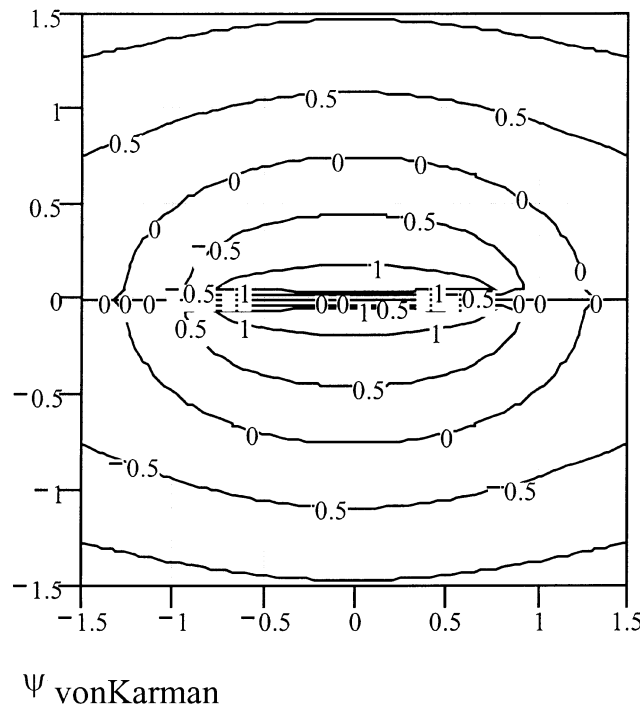


Fig. 9. Illustration of von Kármán’s method: two-dimensional free stream about a series of sources and sinks situated along the x-axis. The streamline $\psi = 0$ represents the outline of the body.

Circle theorem

With the aircraft trailing vortex example, the aircraft centerline was seen to be a plane through which no flow passed; similarly, an aircraft in ground effect also had no flow through the plane that represented the ground. This technique is referred to as the method of images, and is not restricted to plane boundaries. In fact, Milne-Thompson’s circle theorem [23] states that if the complex potential $f(z)$ represents a flow without singularities for $|z| < a$, then:

$$F(z) = f(z) + \bar{f}\left(\frac{a^2}{z}\right) \tag{19}$$

represents the same flow at infinity with a circle of radius ‘ a ’ at the origin. (When used on a function, the overbar notation \bar{f} indicates that all complex constants in the original function f are now their complex conjugates.) In the case of a vortex situated at z_{real} in the vicinity of a circular cylinder of unit radius, the circle theorem gives the complex potential:

$$F(z) = \frac{-i\Gamma}{2\pi} \ln(z - z_{real}) + \frac{i\Gamma}{2\pi} \ln\left(\frac{1}{z} - \bar{z}_{real}\right) \tag{20}$$

Following a bit of algebra, this equation may be recast as:

$$F(z) = \frac{-i\Gamma}{2\pi} \ln(z - z_{real}) + \frac{i\Gamma}{2\pi} \ln\left(z - \frac{1}{\bar{z}_{real}}\right) - \frac{i\Gamma}{2\pi} \ln z + \frac{i\Gamma}{2\pi} \ln(-\bar{z}_{real}) \tag{21}$$

Studying the right hand side of this last equation reveals that the first term is the real vortex; the second term is an image vortex of equal (but opposite) strength situated at $1/\bar{z}_{real}$; the third term is a vortex of the same magnitude and sense as the real vortex, but located at the origin; the last term is a constant which ensures that the locus of $\psi = 0$ coincides with $|z| = a = 1$. Had the last term been left off, there would still be a circular streamline on $|z| = a = 1$, but its value would be non-zero. It is a simple matter to plot the resulting streamlines using either of the last two equations in MathCad; additionally, if the second equation is used, the change in streamline values which occurs when the last term is included or left out can be readily and quickly observed.

Figure 10 illustrates either of the last two equations with $\Gamma = 2\pi$ and $z_{real} = 1.2 + 1.2i$; note that the image vortex is located at $z_{image} = 1/\bar{z}_{real} = .417 + .417i$ on a line between the origin and the real vortex. Students should be encouraged to invoke the circle theorem for multiple vortices to simulate the classic Kármán vortex street, or to verify the validity of the circle theorem when applied to sources, sinks, and/or doublets.

Kelvin oval

Numerous other possibilities for further study may be found in the references [24–26] or in the current literature. As a final illustrative example, though, the Kelvin oval is shown in Fig. 11. This results from a vortex pair of equal magnitude and opposite sign whose axis is perpendicular to an

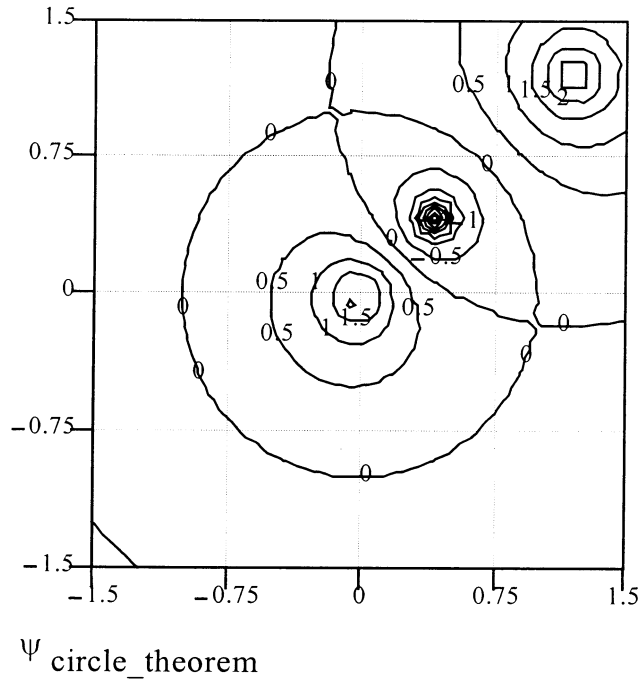


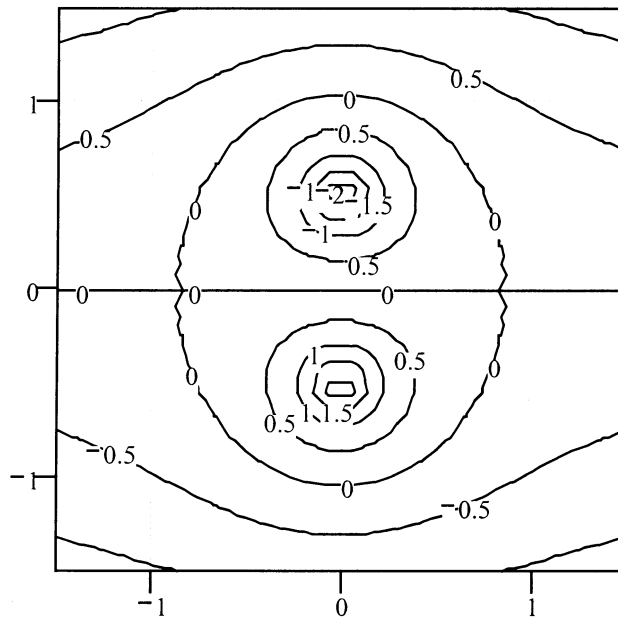
Fig. 10. Illustration of the circle theorem for a real vortex of strength $\Gamma = 2\pi$ situated at $z = 1.2 + 1.2i$ in the presence of a cylinder of unit radius centered on the origin.

opposing free stream, resulting in a complex potential of:

$$F(z) = U_0 z - \frac{\hat{i}\Gamma}{2\pi} \ln\left(\frac{z - z_{\text{upper}}}{z - z_{\text{lower}}}\right) \quad (22)$$

where $z_{\text{upper}} = \hat{i}/2$, $z_{\text{lower}} = z_{\text{upper}}$, $U_0 = 1$, and $\Gamma =$

2π . It can be seen that this constitutes a recirculation cell within the streamline $\psi = 0$. In fact, if the vortices are brought together in such a manner that the product of their strength and spacing approaches a finite value, a doublet results, just as was obtained from a similar source/sink combination. The only difference is that the vortex pair is



Ψ Kelvin_Oval

Fig. 11. Streamlines of Kelvin oval representing from free stream opposing the flow from two oppositely-signed vortices of magnitude 2π located at $z = \pm(i/2)$.

oriented perpendicular to the free stream, while the source/sink combination lies on an axis parallel to the free stream.

CONCLUSION

MathCad is an inexpensive and readily available calculation software package which, even in the student version, contains a powerful contour plotting routine and the ability to perform calculations with complex numbers. These features make it an

excellent choice for teaching ideal fluid flow with complex variables. The lesson plan provided on the MathCad web site may be easily modified to suit individual teaching preferences or topics. With minimal effort, the lesson plan may be changed to provide instruction in electrostatics. The stream function ψ for the fluid flow problem is analogous to the potential function in the electrostatic analog; likewise, the potential function ϕ (and the equipotentials) of the fluid flow problem find their parallels in the stream function (and lines of force) of electrostatics.

REFERENCES

1. G. J. Hokensen and R. D. W. Bowersox, Flow visualization, in *Handbook of Fluid Dynamics and Fluid Machinery, Volume II: Experimental and Computational Fluid Dynamics*, ed. J. A. Schetz and A. E. Fuhs, Wiley, New York, (1996) pp. 1019–1039.
2. B. Carr and V. E. Young, Videotapes and movies on fluid dynamics and fluid machines, in *Handbook of Fluid Dynamics and Fluid Machinery, Volume II: Experimental and Computational Fluid Dynamics*, ed. J. A. Schetz and A. E. Fuhs, Wiley, New York, (1996) pp. 1171–1189.
3. J. C. Bruch, Jr. and R. C. Wood, The teaching of hydrodynamics using computer generated displays, *Bull. Mech. Engng. Educ.*, **9**, (1970) pp. 105–115.
4. D. R. Broome, Interactive graphics display of inviscid fluid flows developed using conformal transformations, *IJMEE*, **6** (4), (1978) pp.191–195.
5. J. C. Bruch, Jr., The use of interactive computer graphics in the conformal mapping area, *Computers & Graphics*, **1**, (1975) pp. 361–374.
6. R. C. Wood and J. C. Bruch, Jr., Teaching complex variables with an interactive computer system, *IEEE Transactions on Education*, **V-15** (1), (Feb 1972) pp. 73–80.
7. J. Mittleman and A. K. Mitra, Exploring two-dimensional potential flow on a personal computer, *Computers in Education Journal*, **IV** (1), (Jan–Mar 1994) pp. 70–76.
8. T. A. Fenaish, Numerical experiments on potential flow configurations, *Computers in Education Journal*, **II** (4), (Oct–Dec 1992) pp. 17–20.
9. R. C. Ertekin and B. Padmanabhan, Graphical aid in potential flow problems: computer program POTFLO, *Computers in Education Journal*, **IV** (4), (Oct–Dec 1994) pp. 24–31.
10. F. B. Hildebrand, *Advanced Calculus for Applications*, Prentice-Hall, Englewood Cliffs NJ (1962) Ch. 10.
11. E. Kreyszig, *Advanced Engineering Mathematics*, 8th ed., Wiley, New York (1999) Ch. 12.
12. V. L. Streeter, E. B. Wylie and L. W. Bedford, *Fluid Mechanics*, 9th ed., WCB/McGraw-Hill, Boston (1998) Ch. 8.
13. G. Magnus, Über die Abweichung von Geschossen [On the deviation of shots (projectiles)]. *Abh. Der Berlin Akad.*, 1851; Über die Abweichung der Geschosse und Auffallende Erscheinungen bei Rotierenden Körpern, *Ann. Phys.*, **88**, 1853, p. 1.
14. J. W. Strutt, Lord Rayleigh, On the irregular flight of a tennis ball, *Messenger of Math.*, **7** (1877); *Scientific Papers*, **1**, pp. 344–46.
15. W. M. Swanson, The Magnus effect: a summary of investigations to date, *Journal of Basic Engineering, Trans. Am. Soc. Mech. Eng.*, **83D**, (September 1961) pp. 461–470.
16. The Cousteau Society, *Calypso II—A Revolutionary, Environmentally Friendly Ship*, web site <http://www.pilot.infi.net/~merriam/cousteau/page/calyp2.htm> (March 10, 1999).
17. J. K. Harvey and F. J. Perry, Flowfield produced by trailing vortices in the vicinity of the ground, *AIAA Journal*, **9**, (8), (1971) pp. 1659–60.
18. Z. C. Zheng and R. L. Ash, Study of aircraft wake vortex behavior near the ground, *AIAA Journal*, **34** (3), (March 1996) pp. 580–589.
19. T. von Kármán, Berechnung der Druckverteilung an Luftschiffkörpern, *Abhandlungen aus dem Aerodynamischen Institut an der Technischen Hochschule Aachen*, **6**, (1927) pp. 3–17. Translated as NACA TM 574: *Calculation of Pressure Distribution on Airship Hulls*, by M. Miner (July 1930).
20. J. M. Robertson, *Hydrodynamics in Theory and Application*, Prentice-Hall, Englewood Cliffs NJ (1965).
21. C. Y. Chow, *An Introduction to Computational Fluid Mechanics*, John Wiley & Sons, New York (1979) Ch. 2.
22. J. L. Hess, Potential Flow, in *Handbook of Fluid Dynamics and Fluid Machinery, Volume I: Fundamentals of Fluid Dynamics*, ed. J. A. Schetz and A. E. Fuhs, Wiley, New York, (1996) pp. 55–56.
23. L. M. Milne-Thompson, *Theoretical Hydrodynamics*, 5th ed., MacMillan, London (1968).
24. H. R. Vallentine, *Applied Hydrodynamics*, Butterworths, London (1969).
25. J. Katz and A. Plotkin, *Low-Speed Aerodynamics: From Wing Theory to Panel Methods*, McGraw-Hill, New York (1991).
26. H. Glauert, *The Elements of Aerofoil and Airscrew Theory*, 2nd ed., Cambridge University Press, Cambridge (1947).

Michael Rex Maixner graduated with distinction from the United States Naval Academy (1972), and served as a commissioned officer in the United States Navy for 25 years; his first 12 years were spent as a line (shipboard) officer, while his remaining service was spent strictly in engineering assignments. He received his Ocean Engineer and SMME degrees from MIT (1977), and his Ph.D. in mechanical engineering from the Naval Postgraduate School (1994). His military service included 2 years on the faculty at the Naval Postgraduate School. Upon completing his military service in 1997, he accepted a position as Associate Professor of Engineering at Maine Maritime Academy in Castine, Maine.